A spectral entropy method for distinguishing regular and irregular motion of Hamiltonian systems

J. Phys. A: Math. Gen., Vol. 12, No. 11, 1979. Printed in Great Britain

A spectral entropy method for distinguishing regular and irregular motion of Hamiltonian systems

G E Powell and I C Percival

Department of Applied Mathematics, Queen Mary College, University of London, Mile End Road, London E1 4NS, UK

Received 30 January 1979

Abstract. Regular and irregular motions of bounded conservative Hamiltonian systems of N degrees of freedom can be distinguished by the structure of the frequency spectrum of a single trajectory. The spectral entropy S is introduced which provides a measure of the distribution of the frequency components. Numerical calculations on the model Hénon and Heiles system and a realistic molecular model are performed. Power spectra are obtained from numerical solutions to Hamilton's equations using fast Fourier transforms and the Hanning method. For regular trajectories S is found to stabilise after a finite time of integration, while for irregular cases S increases erratically. Estimates of the relative volume of regular regions of phase space as a function of energy are given for the two systems.

1. Introduction

Conservative Hamiltonian systems of a finite number of degrees of freedom exhibit two significant types of bounded classical motion—regular and irregular. Regular and irregular motion may be distinguished by the form of phase space trajectories, or by the structure of the frequency spectra of the motion. A regular trajectory of a system of N degrees of freedom is wound onto an N-dimensional torus in the $2N$-dimensional phase space, and the motion has a discrete frequency spectrum. Almost all bounded trajectories of integrable systems are regular, and this includes all systems which are linear, separable or of one degree of freedom. An irregular trajectory normally wanders throughout a region of phase space of dimension greater than N, and typically throughout a significant fraction of an energy shell of dimension $2N-1$. Its frequency spectrum is not discrete. Irregular trajectories are strongly unstable and are not so well understood as the regular trajectories. For certain systems, such as a particle moving on a surface of constant negative curvature, all bound trajectories are irregular and also ergodic, but this is exceptional (Sinai 1961).

Numerical experiments strongly suggest that, for most systems where bounded motion takes place, motion can be regular or irregular, and both are significant. Those parts of phase space occupied by regular trajectories are named the regular regions, and those parts occupied by the irregular trajectories are the irregular regions (Whiteman 1977). The motion in irregular regions is sometimes called stochastic or unstable motion.

0305-4470/79/112053+19$01.00

Because the motion is so different in the regular and irregular regions, we would like to know the volumes of each for many applications, such as the motion of stars in a galaxy (Contopoulos 1963, 1970, 1971), the motion of particles in accelerators and magnetic traps (Dunnett *et al* 1968), the structure of magnetic field lines in plasma containment devices (Arnol'd 1963), the theory of thermal conductivity, and also the dynamics and vibrational spectra of polyatomic molecules, which are our principal concern (Percival 1973, 1977, Percival and Pomphrey 1976a, b, Noid *et al* 1977, Handy *et al* 1977).

A review of regular and irregular motion is given by Whiteman (1977).

The regular and irregular regions of phase space have a very complicated interleaved structure which makes rigorous estimates of their volume difficult even for the simplest cases. The existence of a regular region of positive volume for an integrable system subject to a slight perturbation is the subject of KAM theory, and the proofs of Arnol'd (1963) and Moser (1962) provide rigorous positive lower bounds on the volume of regular regions for sufficiently small perturbations. But Hénon (1966) has pointed out that the perturbation has to be smaller than 10^{-48} in suitable units for *any* such a bound to be given by these proofs, so the rigorous theory does not yet provide a useful bound.

The theory of overlapping resonances (Rosenbluth *et al* 1966) provides a non-rigorous estimate for the volume of the regular region, but numerical tests show errors of about a factor of 2 (Chirikov 1979) or more, which is not adequate for many purposes.

Estimates based on stepwise numerical integration of trajectories are not rigorous, but they can be useful in practice.

The classical Hamiltonian models of real physical systems are never exact. There is a maximum time T_M which is an approximate measure of the interval over which the model may be considered valid. The Hamiltonian motion need not be considered over a time longer than the time T_M, which can be measured in units of a typical period T_c of the motion of the system. For example, in a linear system T_c would be the shortest fundamental period, and for perturbed linear systems it would vary from this value by a small factor only.

For stars in the galaxy and for molecules T_M/T_c is of the order of a few hundred or thousand. For particles in fields T_M/T_c can have a wide range up to 10^9 or 10^{10}, and for the solar system T_M/T_c is probably of order 10^9.

Strictly the distinction between regular and irregular motion is made over infinite intervals of time. A regular trajectory *always* remains in an N-dimensional torus. But in practice it is not possible to integrate numerically over infinite intervals, nor is it necessary to consider intervals longer than the time T_M of the system under consideration. Over finite intervals which are sufficiently long, most bound trajectories appear to be regular or irregular, with a relatively small number of ambiguous intermediate cases.

The estimation of volumes of regular and irregular regions by integration of trajectories consists of three stages:

(S1) Choice of initial conditions for the sample of trajectories.

(S2) Integration of trajectories.

(S3) Classification of trajectories as regular or irregular.

Each stage may be carried out by a variety of methods which take different times of computation and which introduce different errors. Stage S1 can be performed using standard Monte Carlo methods of sampling in phase space, and stage S2 by one of the many methods of stepwise integration. Stage S3 is not so simple. A standard method

uses the intercepts of the phase space trajectories with Poincaré's surfaces of section (e.g. Hénon and Heiles 1964), and this enables the dynamics to be visualised clearly, but the method is difficult to extend to systems of more than two degrees of freedom. The method of Greene (1968) using closed trajectories also has this problem, as closed trajectories are increasingly difficult to find as the number of degrees of freedom increases. Another method uses the divergence of trajectories with neighbouring initial points in phase space, but this requires the integration of further trajectories to determine whether one trajectory is regular or irregular. Fourier transforms have been used by Noid *et al* (1977) and by Hänsel (1978) to study the properties of regular and irregular trajectories, but the latter uses divergence in order to distinguish them.

We describe a method based on fast Fourier transforms of the motion and on an entropy measure, named the Fourier entropy, which can be used for systems of an arbitrary number of degrees of freedom, but which requires analysis of only one trajectory. A divergence method is used for purposes of comparison, and the methods are applied to the standard Hénon–Heiles potential and to a realistic molecular potential by way of example.

Section 2 describes the Fourier transforms of regular trajectories, introduces the Fourier entropy and explains the numerical method used to obtain it.

In practice numerical integrations have to be performed over a finite time interval. This causes modifications to the transform which make the estimate of the Fourier entropy difficult. The difficulty is overcome by the Hanning method described in § 3.

Section 4 discusses the irregular trajectories and the form of the divergence of their Fourier entropy. In § 5 the method is applied to the standard model Hénon–Heiles potential for purposes of comparison, and to a model potential for a molecule in order to show that the method is practical for a more complicated realistic example.

2. Fourier transforms for regular trajectories

For convenience we define the Fourier transform of a function $f(t)$ to be

$$F(\omega) = \int_{-\infty}^{\infty} \mathrm{d}t f(t) \exp(-\mathrm{i}\omega t) \tag{2.1a}$$

or

$$F(\nu) = \int_{-\infty}^{\infty} \mathrm{d}t f(t) \exp(-2\pi \mathrm{i}\nu t), \tag{2.1b}$$

where ω is the angular frequency and $\nu = \omega/2\pi$ is the frequency. The trajectories and their transforms have to be obtained numerically, and inevitably there are errors. Since the computing time is significant, care must be taken to ensure that each source of error is identified and minimised, given the time available for computation. In practice this leads to an error-matching problem typical of computational physics (Percival 1976).

The functions representing the trajectories extend into the infinite past and future. They are not quadratically integrable, and the numerical estimation of their transforms requires some care. The two types of trajectory, regular and irregular, behave very differently and have different kinds of transform, so we consider them separately.

The regular trajectories are wound onto invariant tori in phase space. They are conditionally periodic, so that any dynamical variable f which is a function of $\boldsymbol{q}$ and $\boldsymbol{p}$,

the generalised coordinates and momenta, depends on time as a function:

$$f(t) = f(\boldsymbol{q}(t), \boldsymbol{p}(t)) = \sum_{s_1,\ldots,s_N} f_{s_1,\ldots,s_N} \exp[\mathrm{i}(s_1\omega_1^{\mathrm{c}} + \ldots + s_N\omega_N^{\mathrm{c}})t]$$

$$= \sum_{\boldsymbol{s}} f_{\boldsymbol{s}} \exp(\mathrm{i}\boldsymbol{s} \cdot \boldsymbol{\omega}^{\mathrm{c}} t), \tag{2.2}$$

where all vectors have dimension N, the number of degrees of freedom. The function $f(t)$ clearly depends on the choice of trajectory. The vector $\boldsymbol{s}$ has integer components, and the summation over $\boldsymbol{s}$ covers all possible integer N-vectors. The vector $\boldsymbol{\omega}^{\mathrm{c}}$ is a characteristic angular frequency vector with components which are the fundamental angular frequencies of the motion.

If $N = 1$, then equation (2.2) is a simple Fourier summation for a periodic function, but for higher dimensions the motion is periodic only for exceptional Hamiltonians or exceptional orbits. For non-linear systems all angular frequencies of the type $\Omega = \boldsymbol{s} \cdot \boldsymbol{\omega}^{\mathrm{c}}$, for arbitrary integer vector $\boldsymbol{s}$, can appear, but for smooth functions $f(t)$ the Fourier coefficients $f_{\boldsymbol{s}}$ decrease rapidly with $|\boldsymbol{s}|$, so that the sum in (2.2) is dominated by a few terms.

It is convenient to label the frequencies Ω which contribute significantly to the sum by a single integer

$$r = \ldots -3, -2, -1, 0, 1, 2, 3, \ldots \tag{2.3}$$

so that Ω_r are in order of increasing frequency. The Fourier sum then becomes

$$f(t) = \sum_r f_r \exp(\mathrm{i}\Omega_r t). \tag{2.4}$$

Because the function $f(t)$ has this form, its Fourier transform can be written

$$F = 2\pi \sum_r f_r \delta(\omega - \Omega_r) = \sum_r f_r \delta(\nu - \nu_r), \tag{2.5}$$

where

$$\nu_r = \Omega_r / 2\pi. \tag{2.6}$$

The regular motion is characterised by a countable number of frequency components and is generally dominated by relatively few of them. A natural measure of the degree of spread over a number of components is the entropy, which we use as a standard measure.

We can think of the quantity

$$P_r = |f_r|^2 / \sum_{r'} |f_{r'}|^2 \tag{2.7}$$

as a probability associated with the frequency component ν_r. The spectral entropy for the dynamical variable f is then defined as

$$S = -\sum_r P_r \ln P_r. \tag{2.8}$$

For a vector variable $\boldsymbol{f}$ it is given by the same expression with

$$P_r = |\boldsymbol{f}_r|^2 / \sum_{r'} |\boldsymbol{f}_{r'}|^2. \tag{2.9}$$

For Hamiltonian systems with a Hamiltonian function of the form

$$H = cp^2 + V(r), \tag{2.10}$$

with p a momentum conjugate to r, we find it particularly convenient to use the entropy of the momentum p, which is the entropy of the power spectrum.

In a numerical integration of trajectories we cannot obtain the coefficients f_r directly, since we do not know the frequencies, and we can only integrate for a finite time. We have to obtain the Fourier transform, which gives an approximation to the expression (2.5) in which the δ functions appear as peaks of finite height.

Any numerical Fourier transform has itself to be approximated by a finite Fourier sum. This is not to be confused with any of the sums above and involves two quite distinct approximations to equation (2.1). They are:

(A1) The infinite integral is replaced by an integral over a finite interval of time $(-T/2, T/2)$.

(A2) The integral over the finite time interval is replaced by a sum over a finite number of points in this interval, normally equally spaced at a fixed distance Δt apart, such that

$$T = M\Delta t, \tag{2.11}$$

where M is a large integer. Normally a simple sum with equal weights is used or the advantage of fast Fourier transform (FFT) methods is lost.

First consider the effect on the transform $F(\omega)$ of the function $f(t)$ caused by the use of a finite, rather than an infinite, time interval. The modified transform is the transform of the product of $f(t)$ and the square pulse

$$g(t) = \begin{cases} 1 & |t| \leqslant T/2 \\ 0 & |t| > T/2 \end{cases} \tag{2.12}$$

The transform is therefore given by

$$\int_{-T/2}^{T/2} \mathrm{d}t\, f(t) \exp(-2\pi \mathrm{i}\nu t) = \int_{-\infty}^{\infty} \mathrm{d}t\, f(t)g(t) \exp(-2\pi \mathrm{i}\nu t) = \int_{-\infty}^{\infty} \mathrm{d}\nu'\, F(\nu - \nu')G(\nu')$$

$$= F(\nu) * G(\nu), \tag{2.13}$$

where the * represents a convolution and

$$G(\nu) = T \sin(\pi\nu T)/\pi\nu T \tag{2.14}$$

is the transform of the square pulse, and approximates the δ function. In the frequency domain the width of $G(\nu)$ is of the order $2\Delta\nu = 2/T$. A term in $f(t)$ of the form $\exp(2\pi \mathrm{i}\nu_0 t)$ of frequency ν_0 is transformed into a constant times $G(\nu - \nu_0)$, which is centred at $\nu = \nu_0$. Two components with frequencies ν_0 and ν_1 which are closer than $2\Delta\nu$ are difficult to distinguish in the frequency domain, where their G functions overlap. The longer the time T, the smaller is $\Delta\nu$, and the finer the detail in the Fourier spectrum that it is possible to distinguish.

The function $G(\nu)$ has many side-lobes (see figure 1(a)) which cause serious difficulties with the numerical estimate of the entropy. Section 3 on the Hanning function shows how these difficulties are overcome.

Given that the form of the transform is smeared out for details finer than about $\Delta\nu = 1/T$, there is little to be gained by tabulating the transform at any mesh finer than

$\Delta\nu$. We therefore choose to tabulate at the points

$$\nu_l = l\Delta\nu = l/T, \qquad l = 0, \pm 1, \pm 2, \ldots . \tag{2.15}$$

Note that $F(-\nu) = F(\nu)^*$, by the reality of $f(t)$.

For a regular trajectory, each member of the Fourier series (2.5) contributes a δ function to the correct Fourier transform and a G function to the approximate Fourier transform. If one of the frequencies ν_r happens to be a multiple of $\Delta\nu$, then the *tabulated* transform will be non-zero at the characteristic frequency only, a perfectly adequate representation of the δ function. However, if ν_r is not a multiple of $\Delta\nu$, there are significant non-zero values over a wide range of frequencies. This inconsistency plays havoc with the estimate of the entropy, but is overcome by the use of the Hanning function.

Now consider the approximation A2 of replacing the Fourier integral (2.13) by a sum over equal intervals of time $\Delta t = T/M$ at the points

$$t_j = -\tfrac{1}{2}T + (j - \tfrac{1}{2})\Delta t, \qquad j = 1, 2, \ldots, M. \tag{2.16}$$

This introduces an artificial frequency cut-off at $\nu_M = 1/\Delta t$, so the value of Δt which should be used is simply determined by the condition that it is the largest Δt for which there are no significant components with frequencies ν_r higher than ν_M. For smooth potentials, where the size of the components decreases rapidly with frequency, this causes no problems.

When both approximations A1 and A2 are made, the Fourier integral reduces to a finite sum

$$F_l = C \sum_{j=1}^{M} f(t_j) \exp(-2\pi \mathrm{i} \nu_l t_j) = C' \sum_{j=1}^{M} f_j \exp\left(-\frac{2\pi \mathrm{i} lj}{M}\right), \tag{2.17}$$

where $f_j = f(t_j)$. The normalising constant C' does not affect the value of the entropy

$$S = -\sum_l P_l \ln P_l, \qquad P_l = |F_l|^2 / \Sigma_{l'} |F_{l'}|^2, \tag{2.18}$$

so for our purposes F_l can be replaced by

$$F_l = \sum_{j=1}^{M} f_j \exp\left(-\frac{2\pi \mathrm{i} l_j}{M}\right), \tag{2.19}$$

which can be evaluated directly by FFT subroutines.

For vector quantities $\boldsymbol{f}$ there is no difference in principle. The $\boldsymbol{F}_l$ are the tabulated Fourier coefficients, and $P_l = |\boldsymbol{F}_l|^2 / \Sigma_{l'} |\boldsymbol{F}_{l'}|^2$ is the probability.

The procedure for determining the entropy is to fix Δt as above, and then to evaluate $S = S(T)$ for a succession of times

$$T = T_m = 2^m \Delta t, \qquad m = m_0, m_0 + 1, m_0 + 2, \ldots . \tag{2.20}$$

For a regular trajectory $S(T_m)$ should stabilise when $2T_m^{-1}$ becomes smaller than the frequency splitting between the two closest significant components. This does not happen, however, unless the Hanning method is used.

It can be seen that a direct method of computation of the F_l using equation (2.17) requires the evaluation of about M^2 products. For $M = 2^m$ with positive integer m, the FFT method requires only about $M \log_2 M$ products, resulting in a saving of a factor of about 100 for $M = 1024$ (Brigham 1974). Using the FFT method, the computing time

taken by the evaluation of the transforms is small by comparison with the time taken by stepwise integration of the trajectories. The more complicated the Hamiltonian, the less important does the time for the transforms become.

3. The Hanning function

In § 2 we found that the use of a finite time interval, approximation A1, which is equivalent to the multiplication of $f(t)$ by the square pulse $g(t)$, replaced a δ function in the transform by a function $G(\nu-\nu')$. This has large numbers of significant side-lobes, decaying as $1/(\nu-\nu')$; see figure 1(*a*). This problem is known as leakage, and makes the entropy very difficult to estimate.

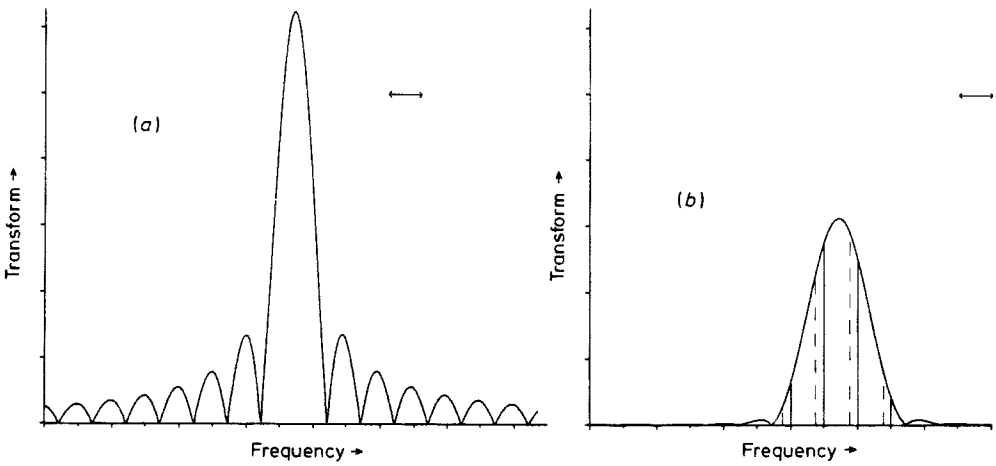

Figure 1. (*a*) The function $|G(\nu-\nu_0)|$ of equation (2.14). The large number of significant side-lobes causes serious difficulties with the numerical estimate of entropy. (*b*) The function $|K(\nu-\nu_0)|$ of equation (3.3). The reduction of the side-lobes compared with $|G(\nu-\nu_0)|$ is evident by comparison with (*a*), which is drawn to the same scale. The double arrows indicate the sample width.

The side-lobes are large because the function $g(t)$ has a sharp cut-off in time. The Hanning method (Brigham 1974) smooths this cut-off and thereby reduces the side-lobes to values so small that they can be neglected. The price is an increased width, which causes few problems. The function $g(t)$ of equation (2.12) is replaced by

$$g(t)h(t) = g(t)\cos^2(\pi t/T) = g(t)\cos^2(\pi\Delta\nu t). \tag{3.1}$$

The Fourier transform of $h(t)$ is

$$H(\nu) = \tfrac{1}{2}\delta(\nu) + \tfrac{1}{4}(\delta(\nu-\Delta\nu)+\delta(\nu+\Delta\nu)) \tag{3.2}$$

and of $g(t)h(t)$ is

$$K(\nu) = G(\nu)*H(\nu) = \frac{1}{2}T\frac{\sin(\pi\nu T)}{\pi\nu T} + \frac{1}{4}\left(T\frac{\sin[\pi(\nu-\Delta\nu)T]}{\pi(\nu-\Delta\nu)T} + T\frac{\sin[\pi(\nu+\Delta\nu)T]}{\pi(\nu+\Delta\nu)T}\right). \tag{3.3}$$

The function $|G(\nu)*H(\nu)|$ appears in figure 1(*b*). The reduction in the side-lobes by comparison with $|G(\nu)|$ in figure 1(*a*) is evident.

The effective width has been doubled to about $4/T = 4\Delta\nu$, but the first side-lobe has been reduced in size to 2% of the peak. The time of calculation is changed negligibly by the change in method.

In § 2 we saw that the calculated entropy of the tabulated transform was very sensitive to the choice of tabulation points. The sensitivity is reduced drastically by the use of the Hanning method, which enables us to obtain accurate estimates of the entropy for regular spectra in which the significant components are separated by at least $4\Delta\nu$ in frequency, using a tabulation interval of $\Delta\nu$.

Consider the function $f(t) = c\exp(2\pi i\nu_0 t)$. Its Fourier transform is $c\delta(\nu-\nu_0)$, and the exact Fourier entropy is zero. The calculated entropy is given by

$$S_{\text{Hann}} = -\sum_l P_l(\nu_0)\ln P_l(\nu_0), \qquad P_l = \frac{K^2(l\Delta\nu-\nu_0)}{\Sigma_{l'} K^2(l'\Delta\nu-\nu_0)}. \tag{3.4}$$

The value of P_l depends on the position of the tabulation points $l\Delta\nu$ with respect to the centre ν_0 of the transform. Two examples are shown in figure 1(*b*).

The entropy S_{Hann} of the function $K(l\Delta\nu-\nu_0)$ has been calculated for a range of values of ν_0, and is found to vary between 0·8633 and 0·8676 with a mean of 0·8655. If we subtract off the mean value we obtain the correct entropy of zero, with an error of at most $2{\cdot}5\times10^{-3}$, which is negligible for our purposes, so S_{Hann} may be considered as a constant,

$$S_{\text{Hann}} = 0{\cdot}8655. \tag{3.5}$$

If the trajectory is regular, the transform consists of a sum over δ functions, so as soon as $4\Delta\nu = 4/T$ is less than the closest distance between two significant δ functions, each δ function is replaced by a K function, each probability P_r is replaced by a set of probabilities

$$P_r \to P_r P_l, \qquad l = -2, -1, 0, 1, 2, \ldots, \tag{3.6}$$

the contribution to the entropy is replaced by

$$-P_r\ln P_r \to -\sum_l P_r P_l(\nu_r)\ln(P_r P_l(\nu_r)) = -P_r\ln P_r + P_r S_{\text{Hann}}, \tag{3.7}$$

and the exact entropy is given by

$$S = S_{\text{calc}} - \sum_r P_r S_{\text{Hann}} = S_{\text{calc}} - S_{\text{Hann}} = S_{\text{calc}} - 0{\cdot}8655. \tag{3.8}$$

Thus we should expect $S(T)$ calculated according to equation (3.8) to vary when $4/T$ is larger than the significant frequency splitting, and then to remain constant. This is found to be the case for trajectories in the known regular regions of Hamiltonian systems.

4. Irregular trajectories

Irregular trajectories are defined as those that are not regular. They do not occupy invariant tori and they are not conditionally periodic. Consequently the Fourier transform of the time variation of a dynamical variable is not a sum over δ functions for

an irregular trajectory. In other words, the Fourier spectrum is not discrete, but there is no evidence that the transform $F(\nu)$ is a continuous function either, except for certain very special cases. There is some numerical indication that $F(\nu)$ is non-zero over finite ranges of the frequency axis. The irregular trajectories defy detailed analysis, but the structure of their transforms and of the Fourier entropy is sufficiently different from the properties of the regular trajectories for the two types of trajectory to be distinguished.

In practice we carry out exactly the same numerical procedure for the irregular trajectories as for the regular trajectories. The calculated time-dependent entropy $S(T)$ does not stabilise for large T, but continues to increase with T or oscillates wildly, and this difference in behaviour is used to distinguish the two types of trajectory.

There are found to be a few ambiguous cases in which the entropy stabilises temporarily and later increases, or in which it oscillates and then stabilises, but the number of such trajectories is not usually very great. We show in the example of the following section that the Fourier entropy method for determining regularity is reasonably consistent with other methods.

Some very special systems are ergodic: all their trajectories are irregular and have a continuous spectrum (Sinai 1961). In this case we can obtain the time dependence $S(T)$ of the Fourier entropy.

Let $\rho(\nu)$ be the normalised power density per unit frequency, so that for constant c

$$\rho(\nu) = c|F(\nu)|^2, \qquad \int_{-\infty}^{\infty} \mathrm{d}\nu \rho(\nu) = 1. \tag{4.1}$$

Then we define the continuous Fourier entropy to be

$$\sum = -\int_{-\infty}^{\infty} \mathrm{d}\nu \rho(\nu) \ln \rho(\nu). \tag{4.2}$$

Unlike the Fourier entropy of a regular trajectory, Σ depends on the units chosen for the frequency, but differences between entropies remain unchanged.

Consider a time of integration T, which is so long that $\rho(\nu)$ varies little within any range f width $\Delta\nu = 1/T$. Then the continuous entropy can be approximated by

$$\sum = -\Delta\nu \sum_l \rho(\nu_l) \ln \rho(\nu_l), \tag{4.3}$$

and $\rho(\nu_l)$ is related to $P_l = P(\nu_l)$ by the differing normalisation conditions

$$1 = \sum_l P_l = \Delta\nu \sum_l \rho(\nu_l), \tag{4.4}$$

$$\rho(\nu_l) = P_l/\Delta\nu = TP_l. \tag{4.5}$$

Therefore for a finite interval T the entropy $\Sigma\,(T)$ is related to $S(T)$ by the expression

$$\sum (\mathrm{T}) = -\sum_1 P_l \ln(TP_l) = S(T) - \ln T. \tag{4.6}$$

In practice we calculate S for both cases, so for a continuous spectrum, in which $\Sigma\,(T)$ is constant for sufficiently large T,

$$S(T) = \sum + \ln T. \tag{4.7}$$

For a continuous spectrum the calculated entropy S does not tend to a constant, but is linear in ln T, with intercept Σ at ln $T = 0$ and slope unity.

For most systems the entropy of the irregular spectrum is not so well-behaved.

5. Applications

The Hamiltonian system described by Hénon and Heiles (1964) was chosen as a test of the theory for several reasons: (i) It is simple analytically which makes the numerical integration fast. (ii) It is sufficiently complicated to exhibit most of the properties of general dynamical systems. (iii) It is well described in the literature (Hénon and Heiles 1964, Churchill *et al* 1978). The Hénon–Heiles Hamiltonian describes a conservative anharmonic system of two degrees of freedom and is of the form

$$H_{\text{H-H}}(q, p) = \tfrac{1}{2}p^2 + U_{\text{H-H}}(q), \qquad (\boldsymbol{q}, \boldsymbol{p}) = (q_1, q_2, p_1, p_2), \tag{5.1}$$

$$U_{\text{H-H}}(\boldsymbol{q}) = \tfrac{1}{2}\boldsymbol{q}^2 + q_1^2 q_2 - \tfrac{1}{3}q_2^3. \tag{5.2}$$

The harmonic approximation without the cubic terms is degenerate. Figure 2 shows a contour plot of the potential function (5.2), which has an escape energy of $\frac{1}{6}$.

Numerical solutions to the equations of motion have been used to determine the regular and irregular regions of phase space. Surfaces of section obtained by Hénon and Heiles (1964) are reproduced in figure 3 for various energies. Regular regions are dominated by continuous closed curves, a sample of which is shown in the figures. Irregular regions are characterised by the erratic scatter of points, through which no simple closed curve seems possible. It has been found (Ford and Lunsford 1970) that this description is oversimplified, but that the large-scale picture remains.

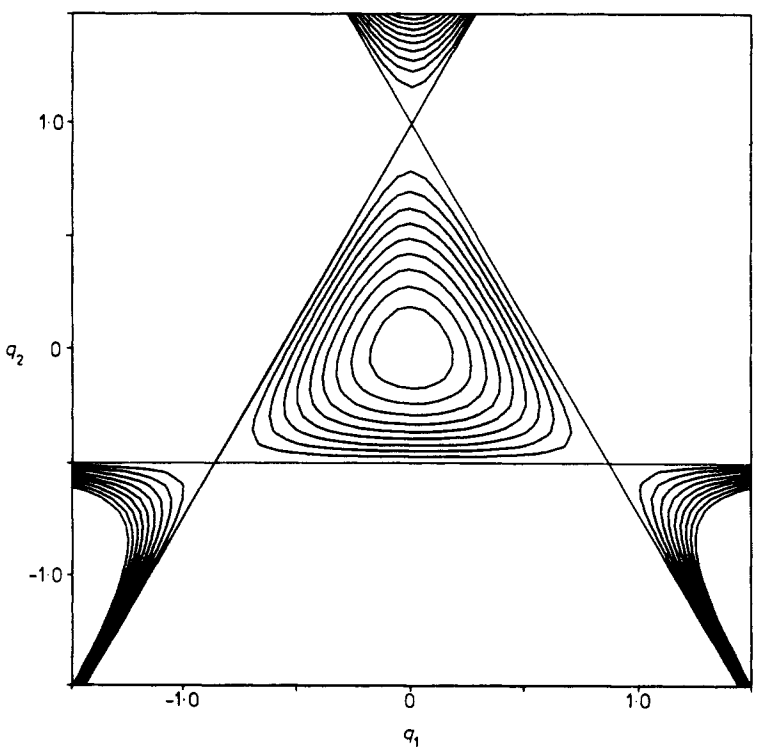

Figure 2. A contour plot of the function $U_{\text{H-H}}$ of equation (5.2). Lines of equipotential are drawn starting near the origin with $U_{\text{H-H}} = \frac{1}{60}$ and increasing uniformly in intervals of $\frac{1}{60}$ to the equilateral contour $U_{\text{H-H}} = \frac{1}{6}$.

As a simple test of the entropy method we investigated ten trajectories with initial points chosen from the surfaces of section (figure 3), some from predominantly regular regions, others from irregular regions. These points are given in table 1 and indicated in figure 3.

Numerical integration of Hamilton's equations of motion was performed over approximately 256 characteristic periods $T_c = 2\pi$ of the unperturbed motion using a Runge–Kutta method. For regular trajectories consistent results were obtained for different step lengths, of approximately 0·01 in units of the characteristic period T_c. Because of the instability of the irregular trajectory, no reasonable interval of integration could be used to give consistent results. However, a theorem quoted by Benettin *et al* (1976) shows that this inconsistency is of little importance, since the numerical errors

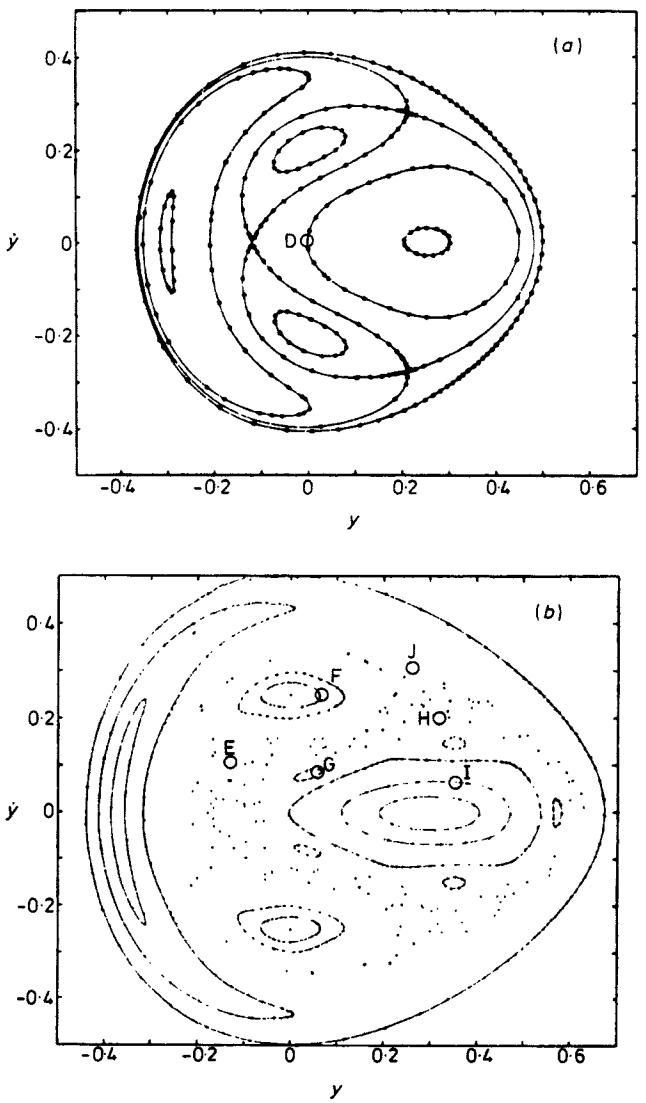

Figure 3(a), (b), see over for (c).

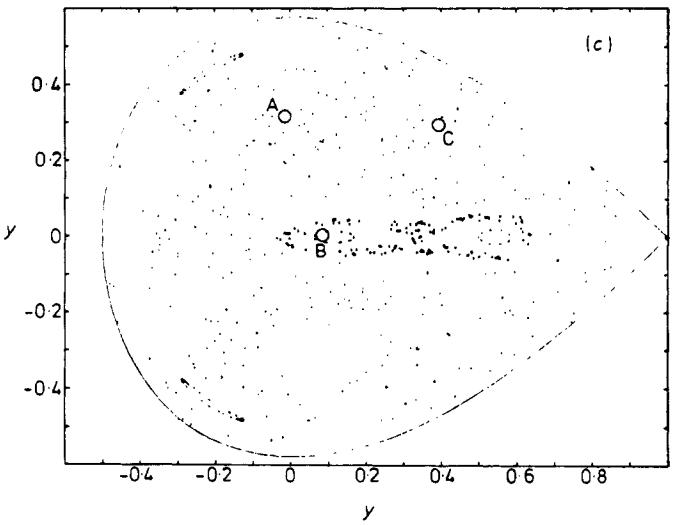

Figure 3. The intercepts of the phase space trajectories for the Hénon and Heiles system (5.1) for energies (*a*) $\frac{1}{12}$, (*b*) $\frac{1}{8}$ and (*c*) $\frac{1}{6}$. The initial points of the ten trajectories are labelled A to J and specified in table 1.

Table 1. Initial values of ten trajectories selected from surfaces of section (figure 3).

Key	x	p_x	y	p_y	Energy
A	0	0·493 295	0	0·3	0·166 67
B	0	0·569 269	0·1	0	0·166 67
C	0	0·370 954	0·4	0·28	0·166 67
D	0	0·408 167	0	0	0·083 30
E	0	0·473 759	−0·12	0·1	0·125 00
F	0	0·433 277	0·07	0·24	0·125 00
G	0	0·488 803	0·07	0·08	0·125 00
H	0	0·359 785	0·32	0·2	0·125 00
I	0	0·390 491	0·35	0·06	0·125 00
J	0	0·322 672	0·26	0·3	0·125 00

have the effect of replacing one irregular trajectory by another one with very slightly differing initial conditions. The instability is used in the divergence method for determining irregularity.

For purposes of comparison with our entropy method we use a divergence measure $D(T)$ defined by

$$D^2(T) = T^{-1}\overline{|\boldsymbol{p}'(t)-\boldsymbol{p}(t)|^2}. \tag{5.3}$$

$D(T)$ is thus the RMS value of the distance in momentum space between two (initially) close trajectories $(\boldsymbol{q}'(t), \boldsymbol{p}'(t))$ and $(\boldsymbol{q}(t), \boldsymbol{p}(t))$ over an interval T. The initial points of the two trajectories differed typically by a factor of 0·999 999.

For regular trajectories the measure is found to increase linearly with time. For irregular cases the rate is more like an exponential. The divergences for the ten trajectories specified by table 1 are shown in figure 4. There is maximum divergence for bounded trajectories corresponding to the size of the energy shell.

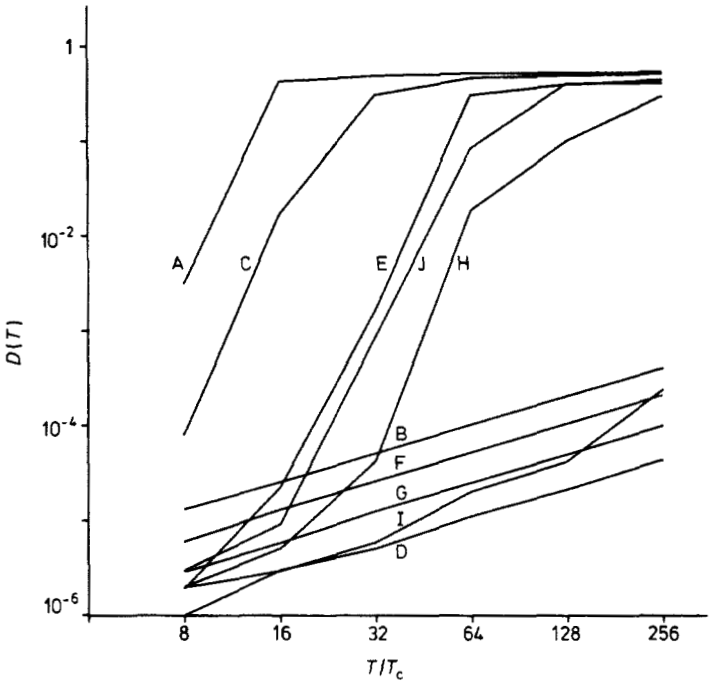

Figure 4. The divergence measure $D(T)$ (equation (5.3)) of the ten trajectories of table 1. For regular trajectories the measure increases linearly with time. For irregular cases the rate is more like an exponential. There is a maximum divergence corresponding to the size of the energy shell.

From these results we label as regular a trajectory for which $D(T)$ varies linearly with T to within 5%,

$$\left|\frac{\Delta(\mathrm{d}D/\mathrm{d}T)}{\mathrm{d}D/\mathrm{d}T}\right| \leqslant 0{\cdot}05. \tag{5.4}$$

For the trajectories B, F, G and D of figures 3 and 4 this quantity is less than 2%.

Power spectra of these ten trajectories were obtained using the now standard FFT routines together with the Hanning modification as described in §§ 2 and 3. The spectra shown in figure 5 are for trajectories of approximately $256T_c$, giving a resolution width $4\Delta\omega \sim 0{\cdot}015$. It can be seen that to this accuracy regular spectra are discrete while irregular spectra are more complicated. Another difference which cannot easily be seen in figure 5 is the small ($\sim 10^{-5}$) but apparently continuous component in the irregular spectrum over much of the frequency domain, which is not present in the regular spectrum ($<10^{-6}$). The main features can be summarised by saying that regular spectra have few, strong components, while irregular spectra have many, weaker components. This has also been observed by Noid *et al* (1977).

The entropy measures determined by the methods of §§ 2 and 3 for the ten trajectories of table 1 are shown in figure 6. The zero component $S_{\mathrm{Hann}} = 0{\cdot}8655$ has been subtracted. It is found that the entropy functions of regular trajectories are constant to within 5×10^{-3} for $T > 64T_c$. According to the results of § 2 this constancy, together with the low value of $S(T)$ itself, is characteristic of regular trajectories. The entropy for irregular trajectories increases erratically with T.

A comparison of the surfaces of section, divergence measures and entropy measures shows good agreement among the three methods for detecting regular and irregular regions of phase space.

There is no need to restrict the energy of trajectories to those of the given surfaces of section. Initial values can be chosen pseudo-randomly with uniform distribution in phase space throughout different energy shells using standard Monte Carlo methods. In this way 100 initial points were chosen subject to the conditions of boundedness

$$q^2 < 1, \qquad U_{\text{H-H}}(q) < \tfrac{1}{6}, \qquad \tfrac{1}{2}p^2 + U_{\text{H-H}}(q) < \tfrac{1}{6}. \tag{5.5}$$

Such trajectories have position coordinates within the equilateral triangle of figure 2, for all time.

A new phenomenon makes its appearance now as a small instability ($\sim 0{\cdot}1$) in the entropy function for six of the eight trajectories with energy less than 0·04. The power

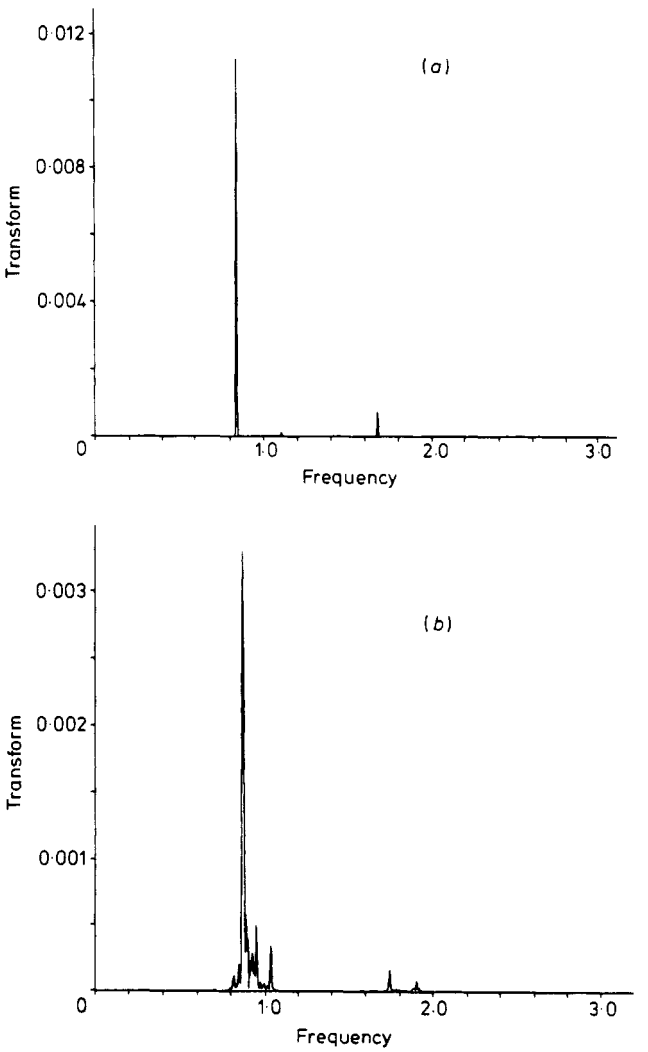

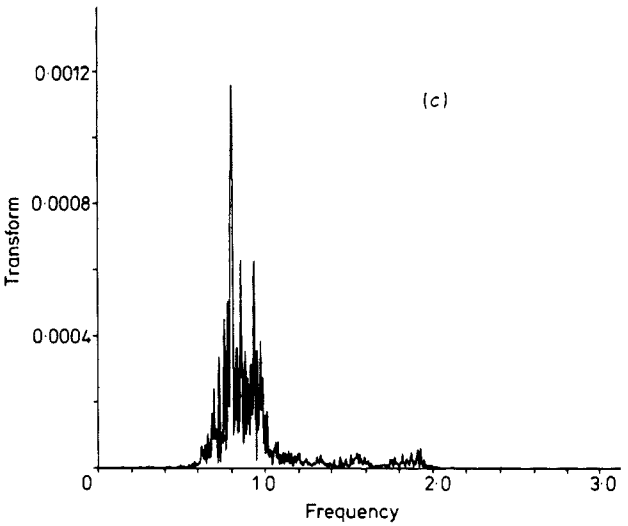

Figure 5. Power spectra for the trajectories (*a*) F, (*b*) J and (*c*) C taken over segments of approximately $T = 256T_c$. The corresponding $K(\omega - \omega_0)$ function has a width $4\Delta\omega = 0{\cdot}015$; to this resolution the spectrum of F is discrete. Conditions (5.4) and (5.6) indicate F is regular, J and C are irregular.

spectra of these six consist of a solitary complex component, appearing as two overlapping components in some cases. The effect can be understood from the approximate degeneracy of the Hamiltonian function (5.1) for small values of energy. The entropy will continue to oscillate until the components are separated. For two close components the entropy function has a maximum of $\ln 2 \simeq 0{\cdot}693$, and this can be used as an alternative condition to be fulfilled by a regular trajectory. We thus label as regular a trajectory whose entropy function satisfies

$$|\Delta S(T)| \leqslant 5 \times 10^{-3} \qquad \text{for} \quad T \geqslant 64T_c \tag{5.6}$$

or

$$S(T) \leqslant 0{\cdot}693.$$

Of the 100 trajectories 95 were found to be described unambiguously and identically in character by the conditions (5.4) and (5.6).

The distribution of regular cases among various energy intervals gives an estimate of the relative volume of regular and irregular regions. Figure 7 shows this estimate calculated by 'binning' the regular and irregular trajectories over the indicated interval of energy. Also shown is the distribution of regular regions obtained by Hénon and Heiles (1964).

The two are not strictly comparable as their estimate is the relative area of regular regions of the corresponding surfaces of section. There is no reason why this should be similar in detail to the ratio of volumes of the full phase space. Also we have found a number of trajectories (ten) irregular according to conditions (5.4) and (5.6) over a period of $256T_c$, but whose divergence over a period of $25T_c$ as used by Hénon and Heiles is that of a typical regular trajectory.

The total computer time for the 100 trajectories was 16 min using a CDC7600. The corresponding time using just the entropy method would be 8 min.

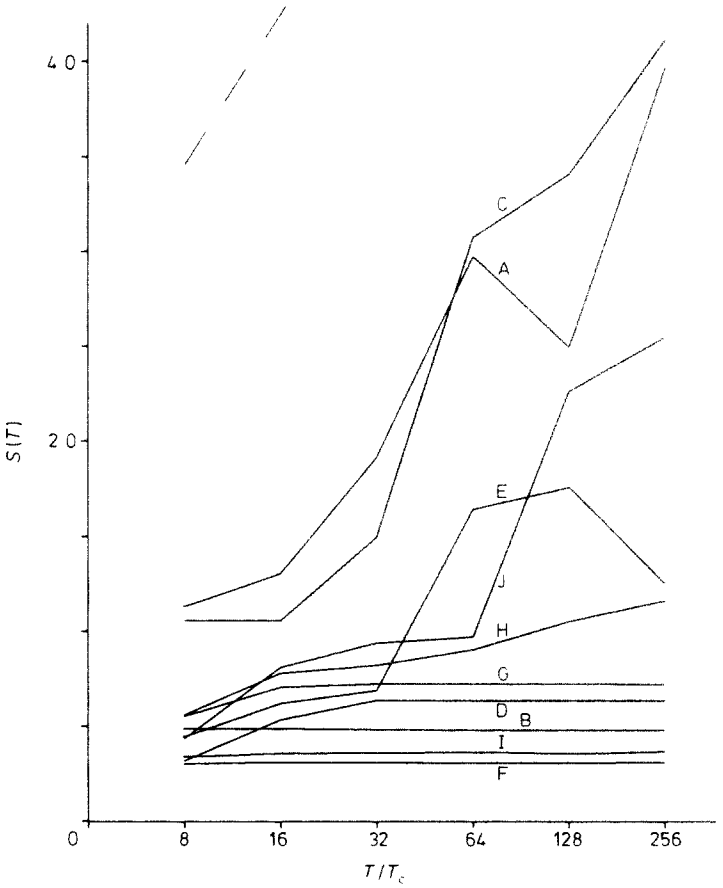

Figure 6. The entropy measure $S(T)$ (equation (3.8)) for the ten trajectories of table 1. $S_{\text{Hann}} = 0{\cdot}8655$ has been subtracted off. $S(T)$ stabilises after approximately $64T_c$. For irregular trajectories $S(T)$ increases erratically. The broken line indicates the maximum limit for $S(T)$.

As mentioned in § 2 both the entropy and the divergence method can be used for systems of more than two degrees of freedom. The final example chosen to illustrate the entropy method is a Hamiltonian system of three degrees of freedom which realistically describes the classical vibrational motion of the linear molecule carbonyl sulphide (OCS). We use the analytic form of Foord *et al* (1975) derived semi-empirically using spectroscopic data, which is

$$H_{\text{FSW}} = \tfrac{1}{2}\sum_{i=1}^{3}(\omega_i p_i^2 + \omega_i q_i^2) + \sum_{i>j>k} k_{ijk}q_iq_jq_k + \sum_{i>j>k>l} k_{ijkl}q_iq_jq_kq_l + k_{22223}q_2^4q_3. \tag{5.7}$$

The corresponding potential function is of a general quartic form with one quintic term to adequately represent the 'Fermi resonance'. Table 2 gives the values of the constants ω and k. The harmonic approximation is not degenerate. This truncated polynomial form is known to give accurate energy levels both quantum mechanically (Foord *et al* 1975) and by semiclassical methods (Percival and Pomphrey 1978) up to

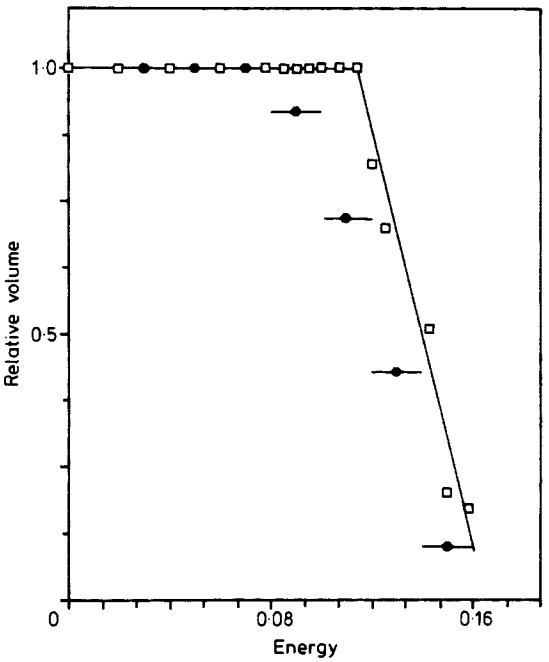

Figure 7. An estimate of the relative volume of regular phase space of the Hénon and Heiles system (5.2), obtained from the ratio of regular trajectories to the total within an energy interval of width 0·02. The full curve is a similar estimate by Hénon and Heiles (1964). As explained in § 5 the two are not strictly comparable.

Table 2. Force constants in the expression for H_{FSW}(4.3)

constant	value	constant	value
ω_1/cm^{-1}	875·70	k_{1113}/cm^{-1}	−4·40
ω_2/cm^{-1}	523·62	k_{1122}/cm^{-1}	−4·95
ω_3/cm^{-1}	2092·46	k_{1133}/cm^{-1}	6·40
k_{111}/cm^{-1}	−33·59	k_{1223}/cm^{-1}	−2·38
k_{113}/cm^{-1}	53·52	k_{1333}/cm^{-1}	0·84
k_{122}/cm^{-1}	42·95	k_{2222}/cm^{-1}	1·77
k_{133}/cm^{-1}	−125·24	k_{2233}/cm^{-1}	−19·28
k_{223}/cm^{-1}	51·30	k_{3333}/cm^{-1}	3·98
k_{333}/cm^{-1}	−67·01	k_{22223}/cm^{-1}	−0·450
k_{1111}/cm^{-1}	1·55		

energies of 5000 in the usual units of cm^{-1}. The energy at which some of the classical trajectories are unbounded is approximately 13 800.

Figure 8 is the corresponding estimate of the relative volumes of regular and irregular regions for the OCS system using the same method as for figure 7. The sample of trajectories used is 150. The full investigation of 150 points took 40 min using a CDC7600.

The indication of a significant irregular region at energies 5000 and beyond is important for comparison with observed vibrational spectra.

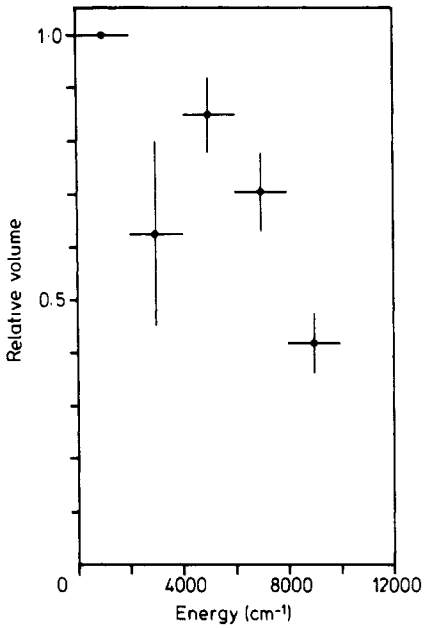

Figure 8. An estimate of the relative volume of regular phase space of the OCS system (5.7), obtained in the same manner as for figure 7. The energy interval here is 2000 cm^{-1}, and the vertical lines represent ± one standard deviation. The anomalous value in the 2000–4000 cm^{-1} interval is caused by the $4\omega_1-\omega_3$ resonance, which is exceptionally small at approximately 2 cm^{-1}. The problem does not occur at the higher energies which are of practical interest, so no effort was made to integrate for longer periods with better statistics to resolve the corresponding regular and irregular orbits.

6. Conclusions

For a classical system of a finite number of degrees of freedom, and for a given dynamical variable and bound classical trajectory, a Fourier entropy S is defined, which is a measure of frequency spread. It converges for regular trajectories and diverges for irregular trajectories. This distinction is used as an effective practical numerical method of distinguishing the two types of trajectory, as illustrated by the well-known Hénon–Heiles potential and by a complicated approximate potential for a triatomic molecule. The FFT and the Hanning technique are essential components of the method.

For finite times T a time-dependent entropy $S(T)$ is defined which converges rapidly to S for long times and regular trajectories, but which diverges for irregular trajectories. Both S and $S(T)$ have a physical significance in the application of semiclassical mechanics to quantal systems.

It is possible that there is a connection between the Fourier entropy and the K entropy (Benettin *et al* 1976), but we have not discovered such a connection.

Acknowledgments

We are grateful to N Pomphrey and D Richards for helpful discussions, and to P Hughes for assistance in the computational work. GP would like to thank the Science Research Council for a research grant.

References

Arnol'd V I 1963 *Usp. Mat. Nauk* **18** (No. 6) 91–192 (Engl. transl. 1963 *Russ. Math. Surv.* **18** 85–191)
Benettin G, Galgani L and Strelcyn J-M 1976 *Phys. Rev.* A **14** 2338
Brigham E O 1974 *The Fast Fourier Transform* (Englewood Cliffs, New Jersey: Prentice-Hall)
Chirikov B V 1979 *Phys. Rep.* **52** 263–379
Churchill R C, Pecelli G and Rod D L 1978 *Preprint* City University of New York
Contopoulos G 1963 *Astrophys. J.* **138** 1297
—— 1970 *Astron. J.* **75** 96
—— 1971 *Astron. J.* **76** 147
Dunnett D A, Laing E W and Taylor J B 1968 *J. Math. Phys.* **9** 1819–23
Foord A, Smith J G and Whiffen D H 1975 *Molec. Phys.* **29** 1685–704
Ford J and Lunsford G H 1970 *Phys. Rev.* A **1** 59
Greene J M 1968 *J Math. Phys.* **9** 760
Handy N C Colwell S M and Miller W H 1977 *Faraday Discuss. Chem. Soc.* **62** 29–39
Hänsel K D 1978 *Chem. Phys.* **33** 35–43
Hénon M 1966 *Bulletin Astronomique, Serie 3* Tome 1, Fascicule 2
Hénon M and Heiles C 1964 *Astron. J.* **69** 73–9
Moser J K 1962 *Nachr. Wiss. Göttingen* **1** 1
Noid D W, Koszykowski M L and Marcus R A 1977 *J. Chem. Phys.* **67** 404–8
Percival I C 1973 *J. Phys. B: Atom. Molec. Phys.* **6** L229–32
—— 1976 in *Atomic Processes and Applications* ed. P G Burke and B L Moisewitsch (Amsterdam: North-Holland)
—— 1977 *Adv. Chem. Phys.* **36** 1–61
Percival I C and Pomphrey N 1976a *J. Molec. Phys.* **31** 97–114
—— 1976b *J. Phys. B: Atom. Molec. Phys.* **9** 3131–40
—— 1978 *Molec. Phys.* **35** 649–63
Rosenbluth M N, Sagdeev R Z, Taylor J B and Zaslavski G M 1966 Nucl. Fusion **6** 297
Sinai Ya G 1961 *Dokl. Akad. Nauk. SSSR* **136** 549–52 (Engl. transl. 1961 *Sov. Math. Dokl.* **2** 106–9)
Whiteman K J 1977 *Rep. Prog. Phys.* **40** 1033–69